

Design and Calibration of Pinch Force Measurement using Strain Gauge for Post-Stroke Patients

Abdallah Alsayed, Raja Kamil*, Hafiz Rashidi Ramli, Azizan As'arry

Faculty of Engineering, University Putra Malaysia, 43400 UPM Serdang, Selangor, Malaysia

*Corresponding Author

DOI: <https://doi.org/10.30880/ijie.2019.11.04.005>

Received 19 April 2019; Accepted 11 July 2019; Available online 5 September 2019

Abstract: Two fingers strength is an indicative measurement of pinch impairment. Conventionally, Fugl Meyer Upper Extremity Assessment (FMA-UE) is the primary standard to measure pinch strength of post-stroke survivors. In literature, the evaluation method performed by the therapist is subjective and exposed to inter-rater and intra-rater reliabilities. Recently, force-sensing resistors were implemented to measure two fingers force, but these sensors are subjected to nonlinearity, high hysteresis, and voltage drift. This paper presents a design of pinch force measurement based on the strain gauge. The pinch sensor was calibrated within a range of between 0 N to 50 N over a pinching length of 20 mm with a linearity error of 0.0123% and hysteresis of 0.513% during the loading and unloading process. The voltage drift has an average of 0.24% over 20 minutes. The pinch force measurement system reveals an objective pinch force measurements in evaluating the rehabilitation progress of post-stroke patients.

Keywords: Post-stroke rehabilitation, Fugl Meyer, pinch force, objective assessment, strain gauge, Arduino Due

1. Introduction

Stroke is a blockage of blood supply to the brain cells which mostly results in the death of brain cells related to motor control [1-3]. Fingers strength is often impaired after stroke [4, 5]. This impairment may cause fingers disabilities, thus limiting hand movements used in daily activities [6]. Fingers performance assessments are of importance in order to facilitate the rehabilitation interventions and monitor the progress of recovery [7, 8]. Clinically, the clinicians assess the pinch strength performance using standard assessments such as FMA-UE, Action Research Arm Test (ARAT), and Wolf Motor Function Test (WMFT) [9]. FMA-UE remains the main tool in research and clinical to evaluate pinch strength impairment [10]. The primary focus of motor evaluation in FMA-UE for hand pinch grasp is to evaluate the patient's ability to grasp a pincer object and exert enough strength against external horizontal pulling [11]. The clinician evaluates the pinch strength manually by exerting pulling force against hand grasp. A pencil is presented to the patient, and he is asked to pinch the pencil between his thumb pad and index pad. The scoring is based on ordinal scale describing three grades of the disability. Grade 0 is given when the patient is unable to independently place his/her thumb and index finger on the pencil that is being held out by the therapist. Grade 1 means that the patient is unable to hold onto the pencil while it is being pulled away. Score 2 is given when the patient is able to hold onto the pencil while it is being pulled away. The patients have to be able to maintain the initial pinch grasp throughout the testing [12].

However, this assessment is based on an ordinal scale which is considered a subjective observation [13, 14]. The evaluation results enormously rely on the tester's experience and skills [15]. In addition, it is costly and timely to find FMA-UE therapist in some countries [16].

Currently, researchers have implemented force-sensing resistors (FSR) and FlexiForce sensors to measure fingers force during the assessment [17]. The outcomes have shown that severe to moderate stroke patients have the difficulty

to wear these sensors [18]. For this reason, clinicians do not support the use of body-worn sensors for patients. A study has shown that FSR and FlexiForce sensors are nonlinear, temperature dependent, high hysteresis, and voltage drift sensor [19]. Therefore, further research has been conducted to study the behavior of these sensors and implement machine learning models to solve the drawbacks. The machine learning models could make the solution complex and costly.

Brimacombe [20] found that the accuracy of the FlexiForce sensor was heavily dependent on calibration procedures and techniques. The recommended approach involves maximizing sensor performance and includes adjusting sensitivity to minimize linearity and repeatability errors, adjusting calibration time to minimize drift, and controlling for temperature. This would maximize the possibility of errors in case of missing one parameter of the recommended process. In addition, the load must be distributed over the sensor area. For instance, a study reported a linearity error of 6% [20]. However, another study showed 4.3% as a linearity error [21]. The calibration process of FlexiForce and FSR is to apply dynamic or static known load on the sensor attached to rigid and flat surfaces underneath. Likitlersuanga [21] and his colleagues studied the FlexiForce on the arm skin. Surprisingly, the accuracy error reached up to $23 \pm 17\%$ based on traditional techniques.

On the other hand, strain gauge provides high linearity, minimal hysteresis, negligible voltage drift, and temperature independent [22]. In addition, they are not body-worn sensors. This paper presents a new design of apparatus to measure pinch strength based on the Fugl Meyer protocol using strain gauge sensing. Firstly, the stress analysis using finite element is performed to determine the location of the strain gauge. Subsequently, standard lab machine is used to calibrate the force against voltage and position. Finally, the force is estimated at unseen positions.

2. Pinch sensor characteristics

2.1 Linearity

Linearity is an important performance concept that describes the response curve of output against the input so as to facilitate the calibration and data processing [23]. In the case of a strain gauge, the linearity refers to the direct proportional relationship between dynamic applied force and voltage of strain gauge resistance. The most common approach, to finding the best line fits between output and input, is the least square method [24]. The least square method is a straight line approximating of the given data. In practice, input and output data does not locate perfectly on the straight line [25]. Deviation of data from the straight line is the linearity error of the calibration process. To find the equation of the line of best fit, consider a set of pairs $(V_1, F_1), (V_2, F_2), \dots, (V_n, F_n)$. Firstly, the mean of the V-values and the mean of the F-values can be calculated using the following formulas:

$$\bar{V} = \frac{\sum_{i=1}^n V_i}{n} \quad (1)$$

and,

$$\bar{F} = \frac{\sum_{i=1}^n F_i}{n} \quad (2)$$

The following equation calculates the slope of the straight line of best fit:

$$S = \frac{\sum_{i=1}^n (V_i - \bar{V}) \times (F_i - \bar{F})}{\sum_{i=1}^n (V_i - \bar{V})^2} \quad (3)$$

Now, the F-intercept of the straight line can be computed as following:

$$b = \bar{F} - S\bar{V} \tag{4}$$

Therefore, the equation of straight line of best fit is:

$$F = b + SV \tag{5}$$

2.2 Hysteresis and voltage drift

Hysteresis is a key parameter to study the performance upon dynamic loadings [26]. It measures the difference in force offset between the force measurements (y-axis) in the loading direction, and the same force measurements in unloading direction at the midpoint in voltage measurements (x-axis) [27]. Fig. 1 shows the variables for hysteresis calculation where V is the voltage, and F is the force. At the midpoint V_m of the curve response, the hysteresis is calculated. The midpoint V_m can be found using the following equation:

$$V_m = \frac{V_{\max} - V_{\min}}{2} + V_{\min} \tag{6}$$

Once the midpoint V_m is located, the two force values (positive and negative going) can be obtained. The following formula calculates the hysteresis.

$$\text{Hysteresis}\% = \left| \frac{F_{mn} - F_{mp}}{F_{\max} - F_{\min}} \right| \times 100\% \tag{7}$$

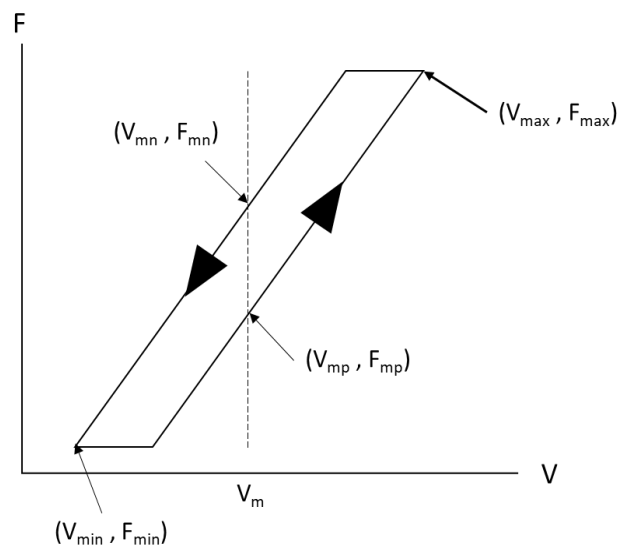


Fig. 1 - Hysteresis diagram explanation

The strain gauge output voltage can be drifted due to temperature, fabrication process, ageing, operating conditions and packaging [28]. This drift limits the accuracy of the strain gauges. The voltage drift can be compensated using compensation algorithms [29]. The most challenging is when the drifting is random. The test of voltage drifting involves recording the output voltage with no load applied over 20 minutes.

3. Experimental procedures

3.1 Design and strain gauge positioning

Fig. 2 shows the typical pinch grasp as in FMA-UE manual. The FMA-UE specialist pulls the pencil away from the patient's grasp with gentle resistance. In this study, the pencil is replaced with a copper alloy of 110 GPa modulus of elasticity. The cylindrical object has a diameter and length of 12 mm and 150 mm respectively. A 4 mm slot is created to allow bending while pinching. A 350 ohm strain gauge (SGK-L1D-K350P-PC11-E) is pasted using instant adhesive (SG401) at the highest stress point during bending. The pinching area is at the beginning of the slot covering finger pad length of 20 mm from the edge of the slot.



Fig. 2 - The clinician (hand on the left) applies horizontal pulling against the patient's grasp (hand on the right) [30]

In this study, ANSYS 15[®] was utilized to perform the stress analysis of the sensor structure. The pinch sensor model is subdivided into small element using meshing function in ANSYS. The meshing is a key procedure in validating the pinch sensor model. Proximity and curvature function distributes the mesh size on faces of the model as seen in Fig. 3. Fig. 4 explains the sizing and inflation settings for meshing. The highest stress point is located at the end of the slot as seen in Fig. 5. For stress analysis, 50 N was applied vertically in $-y$ -axis at the beginning of the slot ($x = 0$ mm). The lower part of the slot is chosen to be the fixed support.

The complete pinch measurement system consists of a pinch sensor, signal conditioning, signal amplification, and microcontroller. The signal conditioning is to measure the variance in strain gauge voltage. Since the change in strain gauge resistance is very small, amplification is needed. The output voltage after amplification is read using a microcontroller.

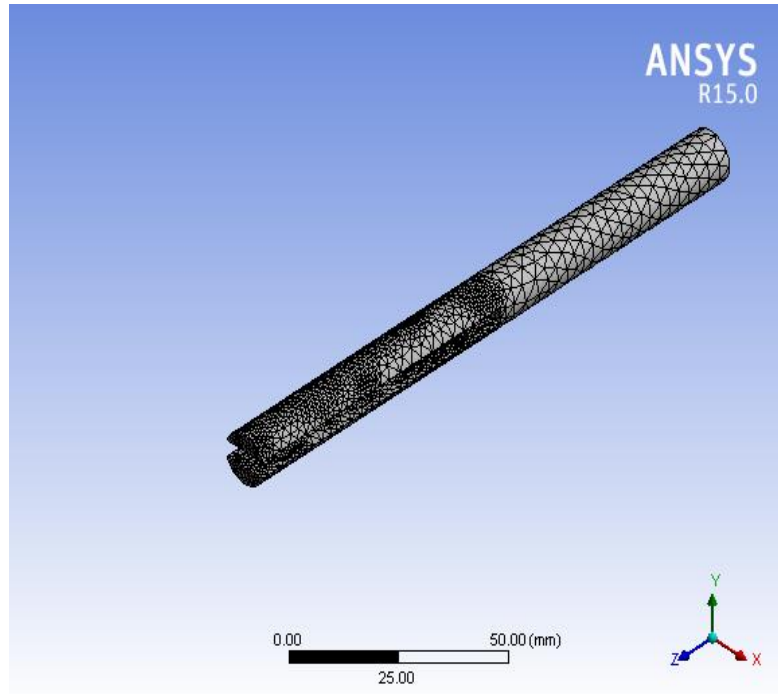


Fig. 3 - Sensor structure meshing

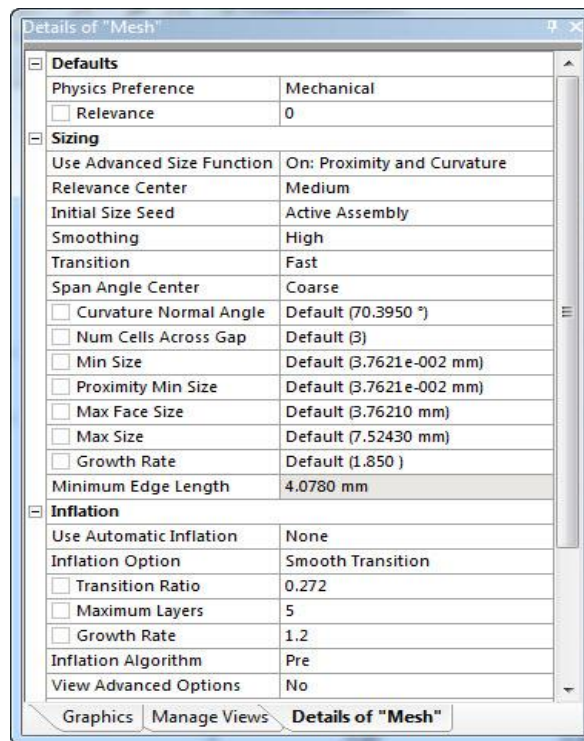


Fig. 4 - Mesh setting used in ANSYS

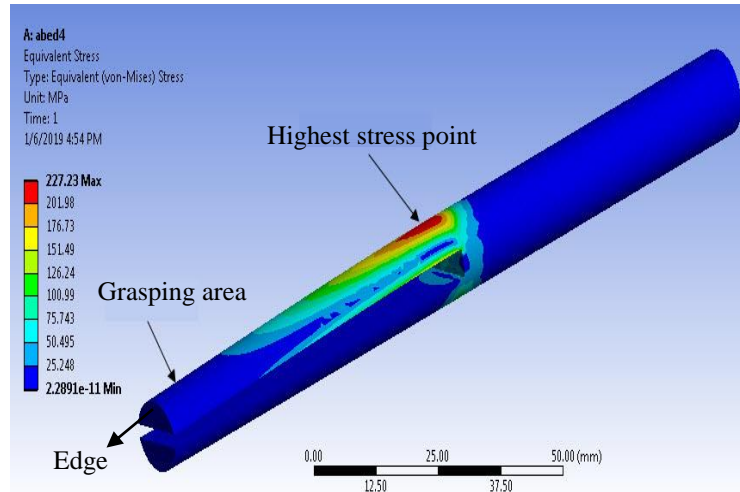


Fig. 5 - FEA stress analysis

3.2 Wheatstone bridge

The Wheatstone bridge is a commonly used as a signal conditioning for strain gauge that consists of four resistors. There are several improvements to Wheatstone bridges with seeking for drift reduction. One approach is to connect a resistor in series with the strain gauge [31] as in Fig. 6. The recommended variable of the resistor is less than the half value of strain gauge resistance (350 Ω); thus we add a 47 Ω resistor (R_4). The structure of the Wheatstone bridge, which is used in this study, is a quarter-bridge. The bridge output voltage (V_{out}) has to be balanced ($V_{out} = 0$) before the calibration. When the load is applied, the strain gauge resistance changes and the bridge output voltage becomes nonzero. The output voltage of the bridge is:

$$V_{out} = \left[\frac{R_{gauge} + R_4}{R_{gauge} + R_4 + R_3} - \frac{R_2}{R_2 + R_1} \right] \times V_{EX} \quad (8)$$

where R_{gauge} is strain gauge resistance, and V_{EX} is the excitation voltage. The value of R_1 is 100 Ω, R_2 is 200 Ω, and R_3 is a variable resistor for output balancing. The excitation voltage is 5 Volts. At balancing ($V_{out} = 0$), R_3 is adjusted to be 198.5 Ω. In practice, it is difficult to have a perfect balancing; therefore, a high quality variable resistor is used.

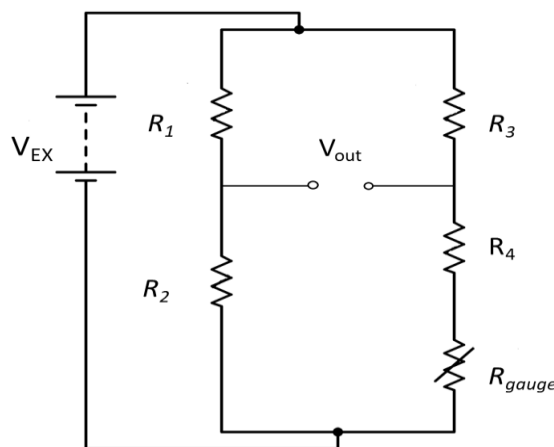


Fig. 6 - Wheatstone bridge circuit

3.3 Force and voltage calibration

To measure very small deformation, the strain gauge is connected to a full Wheatstone bridge with an exciting voltage of 5 Volts generated from the amplifier circuit. The change of Wheatstone bridge voltage is only a few

millivolts; hence an amplifier is required. We have used Wachendorff Strain Gauge Converter® which has a sensitivity of 1 mV and 1000 as a gain. Strain gauge resistance varies due to the applied load and position of the load. Since the patient under FMA-UE test may not precisely hold the pincer object at the pad location, the force may be inaccurate. Therefore, the calibration has to cover the extended length of the possible pinching location. According to [32], the maximum length of the finger pad is less than 20 mm. So, we divided the 20 mm length to six points of calibration (4.4 mm, 6.9 mm, 9.6 mm, 13.5 mm, 17.2 mm, and 20.2 mm).

The calibration process consists of applying dynamic force between 0 N to 50 N at different points covering the pinching length. The dynamic force is applied to six points individually. Four of these points are for calibration, and two points are for validation.

In the lab, the compression universal testing actuator (INSTRON® 3366) was used to apply dynamic compression force with a speed of 3 mm/min. Firstly, we test the hysteresis of the voltage by applying a load (0 N to 50 N) and unload (50 N to 0 N) force at 4.4 mm pinching length position. Then, we apply load force to the rest of the points. The testing actuator gives the data of force, and Arduino Mega provides the data of voltage. Both data must be synchronized before calibration. The synchronization can be done by knowing the sampling frequency of testing actuator microcontroller then adjust it with Arduino sampling frequency. Fig. 7 shows the apparatus of the pinch force measurement system.

4. Results

In the case of zero loads, the average voltage drift of pinch force sensor is 4.8 mV (0.24% of operating capacity) over 20 minutes. The voltage drifting is due to electrical noise such as signal amplification, wiring, Wheatstone bridge, or microcontroller. At 4.4 mm, the loading and unloading forces against voltage relationship are shown in Fig. 8. The equations of loading and unloading curves are:

$$F_{loading} = (0.0216 \times V) + 3.368 \quad (9)$$

and,

$$F_{Unloading} = (0.0214 \times V) + 3.2912 \quad (10)$$

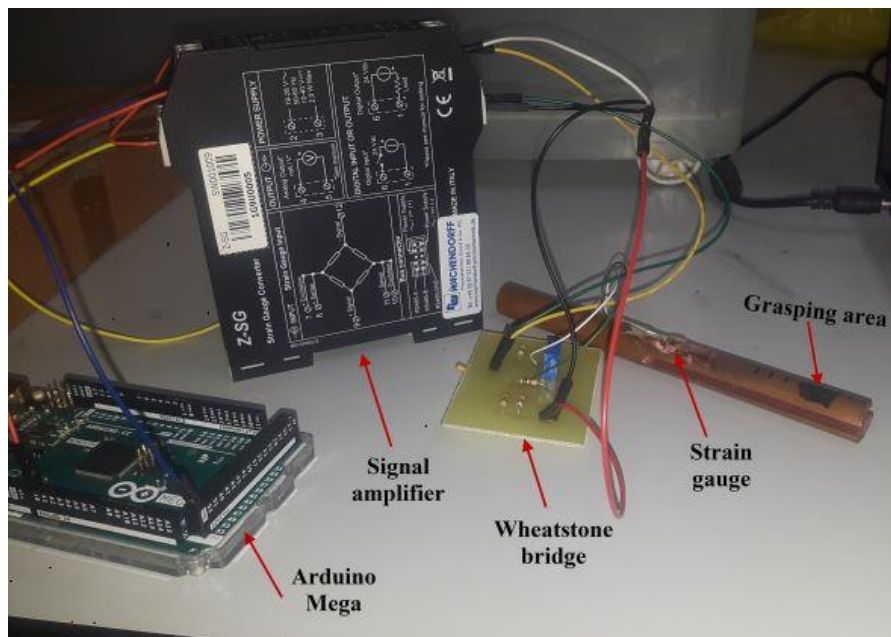


Fig. 7 - Complete pinch force System

where F is the force in Newton, and V is the voltage in mV. The linearity error of loading and unloading forces are 0.0023% and 0.0027% respectively. The hysteresis calculation occurs at the midpoint of the x-axis (voltage = 1042 mV). The two force values, at 1042 mV, of loading and unloading curves, are 25.88 N and 26.12 N respectively.

$$Hysteresis\% = \left| \frac{26.12 - 25.88}{50 - 3.29} \right| \times 100\% = 0.513\% \quad (11)$$

The calibration results of the points (4.4 mm, 9.6 mm, 17.2 mm, and 20.2 mm) are represented in a three-dimensional graph where the x-axis, y-axis, and z-axis represent voltage, position, and force respectively (Fig. 9). The interpolation equation is:

$$F = -0.8975 + (0.02385 \times V) + (0.394 \times P) \quad (12)$$

where F is the force in Newton, V is voltage in mV, and P is position in mm. The linearity error of interpolation is 0.0123%.

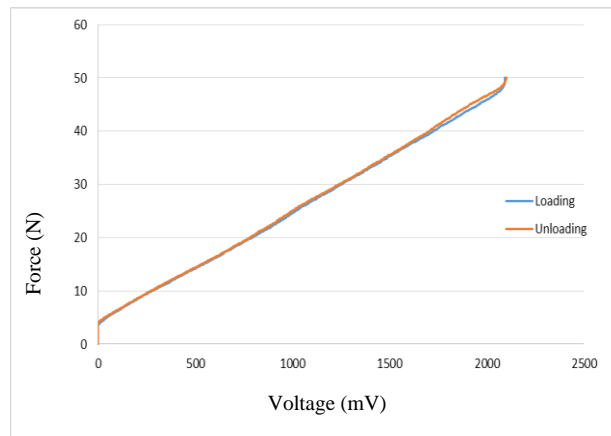


Fig. 8 - Loading and Unloading calibration at 4.4 mm

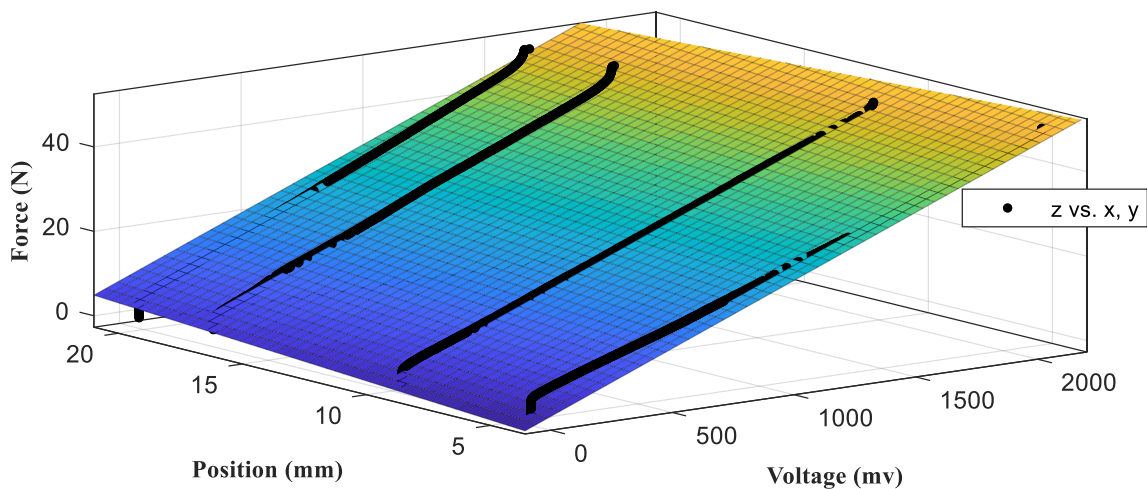


Fig. 9 - Interpolation plane of force as a function of voltage and position

To validate the interpolation equation, we use the two points at 6.9 mm and 13.5 mm for estimation. Table 1 presents a sample of estimated and actual forces. The average error between estimated and actual forces is 3.03% ($\pm 1.52\%$).

Table 1 - Sample of prediction and actual force measurements at two different positions

Voltage (mV)	Position (mm)	Actual Force (N)	Estimated force (N)	Error%
352.44	6.9	11.07	10.56	5.292
538.07	6.9	15.04	14.65	2.657
778.22	6.9	19.98	20.38	1.947
1004.32	6.9	25.01	25.772	2.937
1239.11	6.9	29.97	31.37	4.446
1483.51	6.9	35.03	37.202	5.828
1601.41	6.9	37.8	40.01	5.521
1813.22	6.9	42.37	45.06	5.978
1990.16	6.9	50	49.28	1.45
220.52	13.5	10.1	9.68	4.2
432.77	13.5	15.06	14.743	2.109
642.14	13.5	20.09	19.736	1.782
854.93	13.5	24.93	24.811	0.498
1063.61	13.5	29.97	29.788	0.624
1263.2	13.5	35.07	34.54	1.499
1466.04	13.5	40.04	39.386	1.632
1655.48	13.5	45.04	43.904	2.526
1833.61	13.5	50	48.153	3.69

5. Discussion

One of the gaps in literature is to implement an objective instrument to replace the manual measurement of pinch force based on the Fugl Meyer protocol. The Fugl Meyer protocol states that the object must be a small diameter cylindrical object (pencil, e.g.) for pinching. Besides, the fingers may be slipped during the pulling. Therefore, this study presents a new pinch force sensor, in the shape of a pencil, to accurately measure the force in the case of slippage.

Although Flexiforce sensors have been used in Fugl Meyer protocol, its performance is still ambiguous in term of linearity, voltage drift, and hysteresis. In the manufacturer datasheet, Flexiforce sensors have a linearity error of $\pm 3\%$, voltage drift of 5%, and hysteresis of 5% [19]. But, Lebosse and his team revealed that the linearity error of FlexiForce swings around 5%, hysteresis is 10%, and voltage drift is 6% [33]. Another study reported different characteristics of FlexiForce including linearity (6.5%), hysteresis (5.4%), and drift (2-4%). These variations, in reporting the Flexiforce characteristics, are due to non-standard equipment used in calibration steps and the resistive ink within the sensing area. Comparing to the Flexiforce datasheet, the proposed strain gauge pinch force sensor decreases the linearity error from 3% to 0.0123%, hysteresis from 5% to 0.513%, and drift from 5% to 0.24%.

Strain gauge based pinch force sensor has not yet implemented in the quantification of Fugl Meyer pinch strength assessment yet. Nevertheless, a study reported a strain gauge transducer has been to measure index and long fingers strength [34]. This transducer showed linearity error of 0.37% of full-scale output (27.4 N), and average validation error of 4.06%.

The designed pinch force sensor demonstrates excellent performance including low linearity error (0.0123%), low hysteresis (0.513%), and small voltage drift (0.24%). In addition, the sensor readings are not influenced by temperature change during the calibration and validation process.

6. Conclusion

This paper highlights the subjectivity of the current evaluation of pinch function in FMA-UE assessment. The proposed solution was to design an objective and automated pinch force sensor fits the evaluation requirements. Due to nonlinearity, high hysteresis, and time drift of Flexiforce sensors among skin applications, we have implemented the strain gauge. The design involves a small diameter cylindrical copper object resembling a pencil. The calibration process was to find the relationship between dynamic force, voltage, and position of pinching. The pinch force shows an excellent performance including high linearity (0.9877%), a minimal amount of hysteresis (0.513%), and small voltage drift (0.24%). The interpolation equation of force showed a low linearity error of 1.23%. The validation of the interpolation equation at unseen positions had an average error of 3.03%.

In future work, the force sensor will be mechanically attached to a linear actuator exerting a dynamic pulling force. The linear actuator will provide the objective actuation replacing the therapist's pulling. Besides that, a position sensor will measure the displacement of the pinch grasp while pulling.

Acknowledgement

This work is supported by Universiti Putra Malaysia under the IPS funding no.9574400.

References

- [1] W. Cheah, C. Hor, A. Zariah, and I. Looi. (2016). A Review of Stroke Research in Malaysia from 2000-2014, *The Medical journal of Malaysia*, vol. 71, pp. 58-69.
- [2] H. C. Persson. (2015). Upper extremity functioning during the first year after stroke.
- [3] R. T. Pinzon and R. D. L. R. Sanyasi. (2017). "Complications as important predictors of disability in ischemic stroke," *Universa Medicina*, vol. 36, pp. 197-204.
- [4] K. Baker, L. Barrett, E. D. Playford, T. Aspden, A. Riazi, and J. Hobart. (2016) "Measuring arm function early after stroke: is the DASH good enough?," *J Neurol Neurosurg Psychiatry*, vol. 87, pp. 604-610.
- [5] V. Repšaitė, A. Vainoras, K. Berškienė, D. Baltaduonienė, A. Daunoravičienė, and E. Sendžikaitė. (2015). "The effect of differential training-based occupational therapy on hand and arm function in patients after stroke: Results of the pilot study," *Neurologia i neurochirurgia polska*, vol. 49, pp. 150-155.
- [6] P. C. Deedwania and N. Volkova. (2005). "Current treatment options for the metabolic syndrome," *Current treatment options in cardiovascular medicine*, vol. 7, pp. 61-74.
- [7] G. Kwakkel, B. J. Kollen, and H. I. Krebs. (2008). "Effects of robot-assisted therapy on upper limb recovery after stroke: a systematic review," *Neurorehabilitation and neural repair*, vol. 22, pp. 111-121.
- [8] C. E. Lang, M. D. Bland, R. R. Bailey, S. Y. Schaefer, and R. L. Birkenmeier. (2013). "Assessment of upper extremity impairment, function, and activity after stroke: foundations for clinical decision making," *Journal of Hand Therapy*, vol. 26, pp. 104-115.
- [9] G. M. Johansson. (2015). "Clinical and kinematic assessments of upper limb function in persons with post-stroke symptoms," *Umeå universitet*.
- [10] W. W. Lee, S.-C. Yen, E. B. A. Tay, Z. Zhao, T. M. Xu, K. K. M. Ling, et al. (2014). "A smartphone-centric system for the range of motion assessment in stroke patients," *IEEE journal of biomedical and health informatics*, vol. 18, pp. 1839-1847.
- [11] J. W. Krakauer and S. T. Carmichael. (2017). *Broken Movement: The Neurobiology of Motor Recovery After Stroke*: MIT Press.
- [12] S. J. Page, P. Levine, and E. Hade. (2012). "Psychometric properties and administration of the wrist/hand subscales of the Fugl-Meyer Assessment in minimally impaired upper extremity hemiparesis in stroke," *Archives of physical medicine and rehabilitation*, vol. 93, pp. 2373-2376. e5.
- [13] L. Yu, D. Xiong, L. Guo, and J. Wang. (2016). "A remote quantitative Fugl-Meyer assessment framework for stroke patients based on wearable sensor networks," *Computer methods and programs in biomedicine*, vol. 128, pp. 100-110.
- [14] J. H. van der Lee, H. Beckerman, G. J. Lankhorst, and L. M. Bouter. (2001). The responsiveness of the Action Research Arm test and the Fugl-Meyer Assessment scale in chronic stroke patients.
- [15] S. Amano, A. Umeji, A. Uchita, Y. Hashimoto, T. Takebayashi, K. Takahashi, et al. (2018). Clinimetric properties of the Fugl-Meyer assessment with adapted guidelines for the assessment of arm function in hemiparetic patients after stroke, *Topics in stroke rehabilitation*, vol. 25, pp. 500-508.
- [16] E. J. Woytowicz, J. C. Rietschel, R. N. Goodman, S. S. Conroy, J. D. Sorkin, J. Whitall, et al. (2017). "Determining levels of upper extremity movement impairment by applying a cluster analysis to the Fugl-Meyer assessment of the upper extremity in chronic stroke," *Archives of physical medicine and rehabilitation*, vol. 98, pp. 456-462.
- [17] P. Otten, J. Kim, and S. H. Son. (2015). "A framework to automate assessment of upper-limb motor function impairment: A feasibility study," *Sensors*, vol. 15, pp. 20097-20114.
- [18] S.-H. Lee, M. Song, and J. Kim. (2016). "Towards clinically relevant automatic assessment of upper-limb motor function impairment," in *Biomedical and Health Informatics (BHI), 2016 IEEE-EMBS International Conference on*, pp. 148-151.
- [19] E. R. Komi, J. R. Roberts, and S. Rothberg. (2007). "Evaluation of thin, flexible sensors for time-resolved grip force measurement," *Proceedings of the Institution of Mechanical Engineers, Part C: Journal of Mechanical Engineering Science*, vol. 221, pp. 1687-1699.
- [20] J. M. Brimacombe, D. R. Wilson, A. J. Hodgson, K. C. Ho, and C. Anglin. (2009). "Effect of calibration method on Tekscan sensor accuracy," *Journal of biomechanical engineering*, vol. 131, p. 034503.

- [21] J. Likitlersuang, M. J. Leineweber, and J. Andrysek. (2017). "Evaluating and improving the performance of thin film force sensors within body and device interfaces," *Medical engineering & physics*, vol. 48, pp. 206-211.
- [22] A. Matute, L. Paredes-Madrid, G. Moreno, F. Cárdenas, and C. A. Palacio. (2018). "A Novel and Inexpensive Approach for Force Sensing Based on FSR Piezocapacitance Aimed at Hysteresis Error Reduction," *Journal of Sensors*, vol. 2018.
- [23] T. Yang, D. Xie, Z. Li, and H. Zhu. (2017). "Recent advances in wearable tactile sensors: Materials, sensing mechanisms, and device performance," *Materials Science and Engineering: R: Reports*, vol. 115, pp. 1-37.
- [24] P. Jain, S. M. Kakade, R. Kidambi, P. Netrapalli, and A. Sidford. (2018). "Accelerating stochastic gradient descent for least squares regression," in *Conference On Learning Theory*, pp. 545-604.
- [25] H. Guo, H. He, Y. Yu, and M. Chen. (2005). "Least-squares calibration method for fringe projection profilometry," *Optical Engineering*, vol. 44, p. 033603.
- [26] L. Pan, A. Chortos, G. Yu, Y. Wang, S. Isaacson, R. Allen, et al. (2014). "An ultra-sensitive resistive pressure sensor based on hollow-sphere microstructure induced elasticity in conducting polymer film," *Nature communications*, vol. 5, p. 3002.
- [27] J. Meyer, B. Arnrich, J. Schumm, and G. Troster. (2010). "Design and modeling of a textile pressure sensor for sitting posture classification," *IEEE Sensors Journal*, vol. 10, pp. 1391-1398.
- [28] T. Ando, "Modeling of Pt8W alloy high temperature strain gauge for drift behavior prediction," 2017.
- [29] T. Tanemura and T. R. Vandermeijden. (2018). "Full-bridge strain-gauge array of finger thermal compensation," ed: Google Patents.
- [30] S. M. Michaelsen, A. S. Rocha, R. J. Knabben, L. P. Rodrigues, and C. G. Fernandes. (2011). "Translation, adaptation and inter-rater reliability of the administration manual for the Fugl-Meyer assessment," *Brazilian Journal of Physical Therapy*, vol. 15, pp. 80-88.
- [31] J.-B. Avisse and J. Chiron. (2000). "Wheatstone bridge with temperature gradient compensation," ed: Google Patents.
- [32] S. M. Pasumarty, S. A. Johnson, S. A. Watson, and M. J. Adams. (2011). "Friction of the human finger pad: influence of moisture, occlusion and velocity," *Tribology Letters*, vol. 44, p. 117.
- [33] C. Lebosse, P. Renaud, B. Bayle, and M. de Mathelin. (2011). "Modeling and evaluation of low-cost force sensors," *IEEE Transactions on Robotics*, vol. 27, pp. 815-822.
- [34] G. J. Byers, B. S. Goldstein, and J. E. Sanders. (1998). "An electromechanical testing device for assessment of hand motor function," *IEEE Transactions on Rehabilitation Engineering*, vol. 6, pp. 88-94.